

# System Integration of a Star Sensor for the Small Earth Observation Satellite RISING-2

By Toshinori KUWAHARA, Steve BATAZZO, Yoshihiro TOMIOKA, Kazufumi FUKUDA,  
Yuji SAKAMOTO, and Kazuya YOSHIDA

*Department of Aerospace Engineering, Tohoku University, Sendai, Japan*

(Received June 19th, 2011)

Tohoku University is now finishing the development of its second 50-kg class Earth observation microsatellite RISING-2. RISING-2 is equipped with four camera systems with eight different imaging sensors, including a 5-m ground resolution cassegrain mirror telescope with three fixed wavelength filters in red, green, and blue, as well as a liquid crystal tunable filter. RISING-2 aims to achieve agile high resolution multi-spectral Earth observations. For this mission, Tohoku University has been developing a precise and agile attitude control system including multiple sensors and actuators. The pointing error is required to be less than 0.1 deg and the pointing knowledge shall be better than 0.06 deg. The designed star sensor is based on CCD image sensor which has a flight heritage by the university's first satellite RISING. This system utilizes a pyramid algorithm for secure constellation identification and works with a maximum update frequency of 2 Hz. Its availability is also very high in terms of the satellite's operating angular velocity. In this paper, the system integration of the star sensor as well as the results of its ground based performance evaluation is described in detail.

**Key Words:** Micro Satellite, Earth Observation, Scientific Mission, Star Sensor, Attitude Determination and Control

## Nomenclature

- b** : star vector in camera coordinates
- r** : star vector in reference coordinates
- $C_y, C_z$  : Estimated star position on focal plane [m]
- f** : Focal length [m]

## 1. Introduction

Tohoku University and Hokkaido University are now finishing the development of a new 41-kg microsatellite RISING-2. This satellite inherits the technologies of predecessor RISING (SPRITE-SAT) developed by the Tohoku University and launched in January 2009. RISING-2 is equipped with 4 camera systems with eight different imaging sensors in total, including a 5-m ground resolution cassegrain mirror telescope (HPT), a pair of Sprite (lightning) observation cameras, a bolometer, and a wide angle camera. The HPT has three fixed wave-length filters in red, green, and blue, as well as a liquid crystal tunable filter. With all of these instruments, RISING-2 aims to achieve high resolution multi-spectral Earth observations, stereoscopic observation of cumulonimbus clouds, and image acquisition of the transient luminous events such as Sprite phenomena. In order to achieve these mission objectives, a precise 3-axis stabilized attitude control system is also developed at the Tohoku University, including multiple sensors and actuators such as star sensors and reaction wheels. The orbit of RISING-2 is supposed to be sun-synchronous with an altitude of about 700 km. The engineering model of the system is already developed and successfully tested for performance evaluation and the development of the flight model is now being completed.

The observation targets and associated mission instruments

of the RISING-2 are summarized in Fig. 1 and their configuration is illustrated in Fig. 2. The primary mission is Earth observation with a resolution of 5 meters by using a cassegrain reflector telescope with the diameter of 100 mm and the focal length of 1 m. The visible infrared and multi-spectral images of cumulonimbus clouds can be observed by using a liquid crystal tunable filter (LCTF) as well as usual color images. By continuously observing the cloud images with an interval of about several 100 ms, the detail structure of cumulonimbus clouds in multi-spectrum can be constructed. This resolution is higher than images obtained by conventional satellites such as TRMM, which have 2 km resolution, and ground radar observatories. These observations are expected to solve a mechanism of guerrilla heavy rain and contribute to the establishment of basic technology for weather forecasting.

The RISING-2 also observes the horizontal structure of Sprite which is one of lightning discharge phenomena. In the same years, several similar missions such as TARANIS, ASIM, and JEM-GLIMS are scheduled. The multiple observations in several missions will have the marvelous influence on the science of atmospheric electricity in the meteorology, the space and terrestrial physics, and the gamma-ray astronomy.

The RISING-2 can observe the designated position around the Earth by using the three-axis attitude control system which consists of reaction wheels, star sensors and gyro sensors, etc. The most of the instruments of attitude control system including a central control unit, star sensors and reaction wheels are newly developed in this project by Tohoku University. The accurate pointing control using reaction wheels, gyroscopes, and star sensors is carried out for 15 minutes in sunshine and 15 minutes in eclipse each.

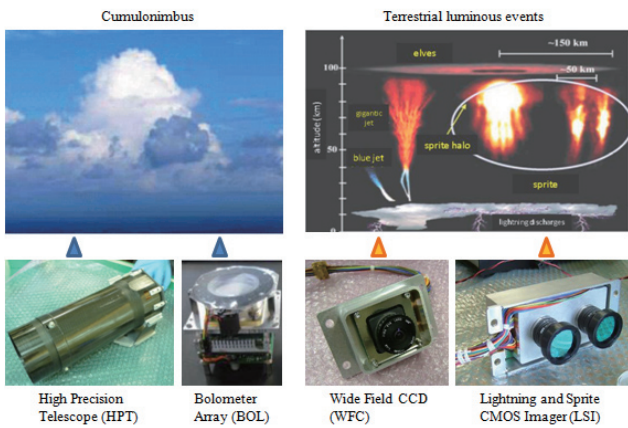


Fig. 1. Mission objectives and scientific instruments.

Another important technical objective of RISING-2 project is to develop the 3-axes stabilized attitude determination and control system. The sensor and actuator components of the attitude control system are summarized together with the satellite system electrical architecture in Fig. 3. Most of these components are based on commercial off the shelf (COTS) components and were integrated by Tohoku University. In this paper, the system integration of the star sensor is described in detail.

## 2. Principles of Star Identification Mechanism

The star sensor attitude determination starts with an astronomical camera designed to capture images of the stars. The next stage is centroiding, the process of detecting the stars in the captured image, and measuring their precise locations. The third stage is the star identification algorithm, which determines which cataloged stars can be found in the image. With some stars identified, the vectors pointing to the stars in the image can be related to their corresponding vectors in celestial coordinates, giving the attitude of the camera. In this chapter, the operation of these system components, especially

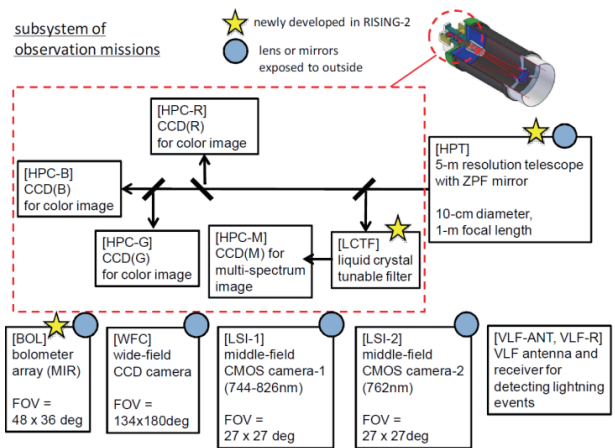


Fig. 2. Mission instruments configuration.

star identification and quaternion calculation, is explained.

### 2.1. Star identification algorithm

For this research, the Pyramid Star Identification Technique published by D. Mortari of Texas A&M University<sup>1)</sup> is chosen. Mortari has published a survey of star identification algorithms<sup>2)</sup>, and the Pyramid Technique shows promise as a quick and efficient way to autonomously identify stars. The reason for this is the range search technique which completes much of the search results before runtime, minimizing the search time while the system is online. In addition, Mortari claims this technique to have high robustness to noise; the original paper claims correct identification with as few as four real stars and as many as 24 random spikes in simulated images. In this paper, the noise robustness is examined more closely. Mortari's paper shows an analytical analysis of the probability of incorrect matches for sets of two, three, and four stars. The conclusion is that a four-star polygon pattern is sufficiently unlikely to generate a false match (on the order of  $10^{-6}$  or less). Thus a four-star pattern is used as a basis for operation, and the sensor should be designed such that at least four stars can be detected in any field of view about the celestial sphere to ensure successful attitude determination.

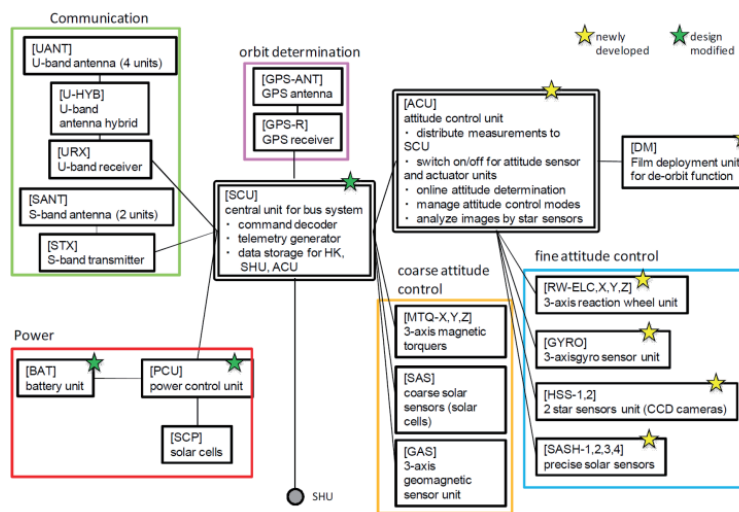


Fig. 3. System electrical configuration.

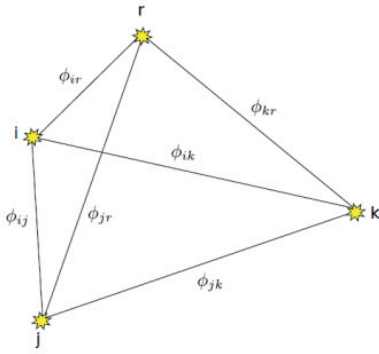


Fig. 4. Pyramid Star Pattern.

This technique uses the angular separation measured between the detected stars to perform pattern matching against a database constructed prior to algorithm execution. The four star polygon pattern, as shown in Fig. 4, consists of six segments; three to compose the base triangle, and three connecting the fourth star to each point on the triangle. First, all possible triangle patterns are checked and if a unique triangle is found the remaining stars are used to check if a fourth star can be matched. If matches are found for the fourth star, then the identification algorithm is considered to be complete. In the original paper, the probability of a false match based on the measured polygon is used as an additional matching criterion; in this implementation, a matched four star pattern is assumed sufficient.

## 2.2. Catalog and lookup table

The catalog contains all pairs of stars which may fit within the camera's field of view. The pairs are recorded in order of angular separation to facilitate efficient searching. Each pair entry contains simply the two star IDs which make up the pair. A range search lookup table can then be constructed. For each measured pair separation angle, the lookup table points to a location in the main catalog where a list of candidate pairs can be retrieved. This saves us from having to search the entire catalog for each measured pair.

## 2.3. Pattern matching

The algorithm starts by trying to find a unique match for a triangle with indices  $i, j, k$ . Starting with any two of the three segments, pairs are sought which share a common pivot point. Until a pivot point is found, the remaining pair is not searched to minimize wasted processing. The order is arbitrary, but this system first looks for a common ID between candidate pairs for segments  $ij$  and  $ik$ . When this is found, the common star is assumed to be star  $i$ , and the remaining stars of each candidate pair must be  $j$  and  $k$  respectively. These are then checked against the star IDs of candidate pairs for segment  $jk$ . If a match is found, a closed triangle is formed. All other potential  $ij$  and  $ik$  matches are checked (followed  $jk$  when a pivot point is matched), and the next step is executed only if the triangle is found to be unique. Once a unique triangle is found, a fourth star  $r$  is chosen and the legs connecting  $r$  to each of the base triangle stars  $i, j$  and  $k$  are identified. A match is accepted if all three of these legs contain the same ID for  $r$ , and match  $i, j$ , and  $k$  respectively. When a four star polygon is matched in this manner, it is accepted as a positive identification.

## 3. Measurement and Calculations

### 3.1. Centroiding

Before executing the pattern matching algorithm, a centroiding filter is needed to detect and locate the stars in the image. Static  $5 \times 5$  windows are used, and all windows in the image are checked (Fig. 5). The criteria for detection of a star in a window are: 1) the sum of the pixels in the window exceeds a certain threshold value and 2) the central pixel is the brightest in most cases. The centroid is then the center of mass of luminosity in the window, and lies somewhere within the central pixel. In this system, a coordinate system is used which matches with celestial polar coordinate system (declination, right ascension). The optical axis is defined as the  $x$ -axis and the image plane is taken to be the  $yz$ -plane. Right ascension (yaw) is rotation about the  $z$ -axis, declination (pitch) is rotation about the  $y$ -axis and finally roll is rotation about the  $x$ -axis. The  $y$  and  $z$  coordinates of a centroid are given as:

$$C_y = \frac{\sum \sum y F(y,z)}{F_{\text{tot}}} \quad (1)$$

$$C_z = \frac{\sum \sum z F(y,z)}{F_{\text{tot}}} \quad (2)$$

where  $F(y, z)$  is the pixel value at  $(y, z)$  and  $F_{\text{tot}}$  is the sum of all pixels in the window.

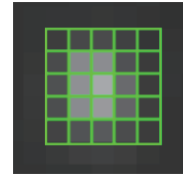


Fig. 5.  $5 \times 5$  centroiding window.

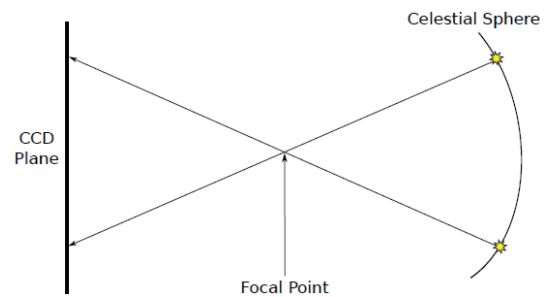


Fig. 6. Celestial sphere projection (pinhole camera model).

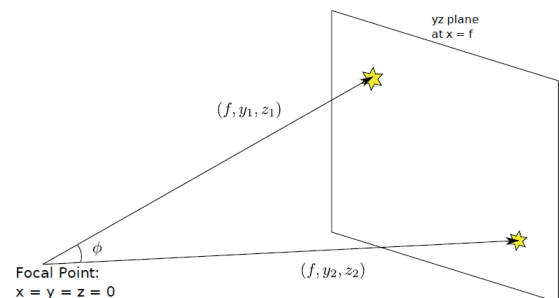


Fig. 7. Vectors pointing to image stars.

### 3.2. Geometry

Though some algorithms make use of relative brightness information, the pattern matching described in the previous subsection is based solely upon the angular separation between each leg of the polygon pattern. It is tempting at first to assume a uniform angular separation per pixel and simply use a value proportional to the linear distance between two detected star centroids. In early simulations with a very small field of view (roughly 3 by 4 degrees), this technique seemed to work reasonably well for star identification. However, with a larger field of view, the algorithm failed or produced incorrect identifications. Replacing this oversimplified model with a pinhole camera model, the imaging system becomes a projection of the celestial sphere onto the flat image plane, which is demonstrated in an exaggerated fashion in Fig. 6. In Fig. 7 two vectors  $(f, y_1, z_1)$  and  $(f, y_2, z_2)$  are shown, each pointing from the focal point of the lens to a star detected on the image plane. The cosine of the angle  $\phi$  between the two stars is simply the dot product of these two vectors:

$$\text{Cos}(\phi) = \frac{y_1 y_2 + z_1 z_2 + f^2}{\sqrt{y_1^2 + z_1^2 + f^2} \sqrt{y_2^2 + z_2^2 + f^2}} \quad (3)$$

To avoid a cumbersome inverse cosine calculation, the result may be left in terms of  $\text{Cos}(\phi)$  and the catalog may be arranged and searched in order of the cosine of the angle between each pair. Mathematically, the cosine of an angle may only fall within the range from zero to one. This is normalized to an integer value for two purposes. First, the dot product measurement result should be used as an array address to fetch catalog information. Second, it is desirable to avoid floating point calculations on the embedded system as much as possible.

### 3.3. Attitude estimation

Once the stars in an image have been identified, we have a set of vectors pointing to the known stars in both the image coordinates and celestial coordinates (stored in the catalog). Since mapping just one vector from one coordinate system to another can yield infinitely many possible orientations (any arbitrary rotation about the result vector satisfies this), at least two vector pairs must be used to completely describe the orientation of the camera. Suppose that the two vectors in camera coordinates are  $\mathbf{b}_1$  and  $\mathbf{b}_2$ , and their corresponding vectors in the reference (celestial) coordinates are  $\mathbf{r}_1$  and  $\mathbf{r}_2$ . This is arbitrarily demonstrated in Fig. 8. We would like an attitude transformation  $\mathbf{A}$  such that:

$$\mathbf{A}\mathbf{r}_1 = \mathbf{b}_1 \quad (4)$$

$$\mathbf{A}\mathbf{r}_2 = \mathbf{b}_2 \quad (5)$$

A simple method of achieving this is presented in Markley<sup>3)</sup>. First, a third vector pair  $\mathbf{r}_3$  and  $\mathbf{b}_3$  are derived by taking the cross products of the two vectors in each frame (Fig. 9).

$$\mathbf{r}_3 = \mathbf{r}_1 \times \mathbf{r}_2 \quad (6)$$

$$\mathbf{b}_3 = \mathbf{b}_1 \times \mathbf{b}_2 \quad (7)$$

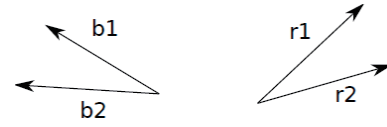


Fig. 8. Vector pairs in two coordinates.

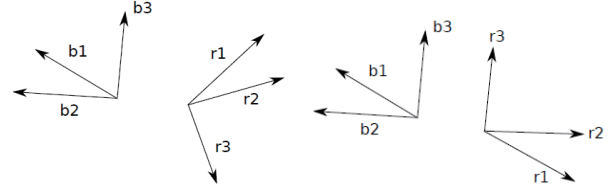


Fig. 9. Quaternion from vectors step1 (left), step2 (right).

Rotating the  $\mathbf{r}$  vectors with the rotation that maps  $\mathbf{r}_3$  to  $\mathbf{b}_3$ ,  $\mathbf{r}_1$  and  $\mathbf{r}_2$  become co-planar with  $\mathbf{b}_1$  and  $\mathbf{b}_2$  (Fig. 9). This rotation is simply a 180 rotation about the vector which bisects  $\mathbf{r}_3$  and  $\mathbf{b}_3$ . The final step is then to rotate about  $\mathbf{b}_3$  by the angle which minimizes the difference between the target and result vector pairs. This angle can be solved analytically. The derivation is left to the reference, but the final quaternion is given as:

$$\mathbf{q}_{\text{opt}} = \frac{1}{2\sqrt{\gamma(\gamma+\alpha)(1+\mathbf{b}_3 \cdot \mathbf{r}_3)}} \begin{bmatrix} (\gamma + \alpha)(\mathbf{b}_3 \times \mathbf{r}_3) + \beta(\mathbf{b}_3 \times \mathbf{r}_3) \\ (\gamma + \alpha)(1 + \mathbf{b}_3 \cdot \mathbf{r}_3) \end{bmatrix} \quad (8)$$

for  $\alpha \geq 0$ , and

$$\mathbf{q}_{\text{opt}} = \frac{1}{2\sqrt{\gamma(\gamma-\alpha)(1+\mathbf{b}_3 \cdot \mathbf{r}_3)}} \begin{bmatrix} \beta(\mathbf{b}_3 \times \mathbf{r}_3) + (\gamma - \alpha)(\mathbf{b}_3 + \mathbf{r}_3) \\ \beta(1 + \mathbf{b}_3 \cdot \mathbf{r}_3) \end{bmatrix} \quad (9)$$

for  $\alpha \leq 0$ , where

$$\alpha = (1 + \mathbf{b}_3 \cdot \mathbf{r}_3)(\mathbf{b}_1 \cdot \mathbf{r}_1 + \mathbf{b}_2 \cdot \mathbf{r}_2) + (\mathbf{b}_3 \times \mathbf{r}_3)(\mathbf{b}_1 \times \mathbf{r}_1 + \mathbf{b}_2 \times \mathbf{r}_2) \quad (10)$$

$$\beta = (\mathbf{b}_3 + \mathbf{r}_3)(\mathbf{b}_1 \times \mathbf{r}_1 + \mathbf{b}_2 \times \mathbf{r}_2) \quad (11)$$

$$\gamma = \sqrt{\alpha^2 + \beta^2} \quad (12)$$

Note that in the reference, weights are given to the different vector measurements corresponding to different measurement uncertainties; for example, this computation may be used to compute attitude from a pair of vector measurements from a sun sensor and a magnetometer. In the case of both input vectors coming from the same star sensor, the vectors may be given equal weights of one.

## 4. Hardware Implementation

The hardware of the star sensor was developed by the Tohoku University based on COTS products. The functionality of the star sensor is divided into two hardware units: data processing electronics and star sensor camera heads as illustrated in Fig. 10, and Fig. 11, respectively. The data processing electronics is also responsible to controlling other types of on-board attitude control system components, such as gyroscopes and reaction wheels as well as conducting attitude



determination and control. Therefore it is named as attitude control unit (ACU). This ACU is based on Xilinx FPGA and SH2 processors together with multiple types of memory chips and can control up to two camera head units.

**4.1. Functional allocation**

The sequence of data processing can be described as followings. The raw image data obtained by a camera head unit is sent to the ACU. The ACU then performs centroiding and star identification in FPGA hardware logic. Then PowerPC processor core inside the FPGA starts processing star catalog mapping and pyramid identification followed by quaternion calculation. The obtained quaternion is finally sent to the SH2 processor for the attitude determination and control purpose.

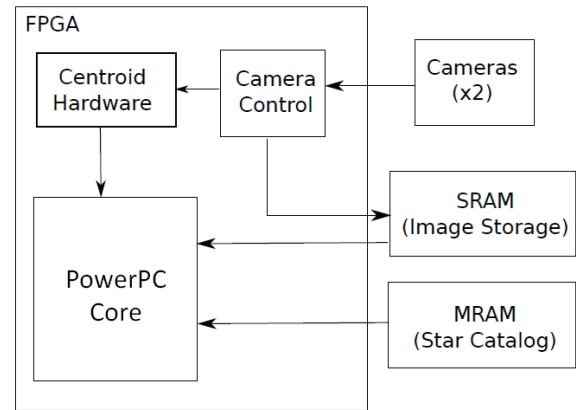


Fig. 12. Internal architecture of the ACU relative to star sensor.

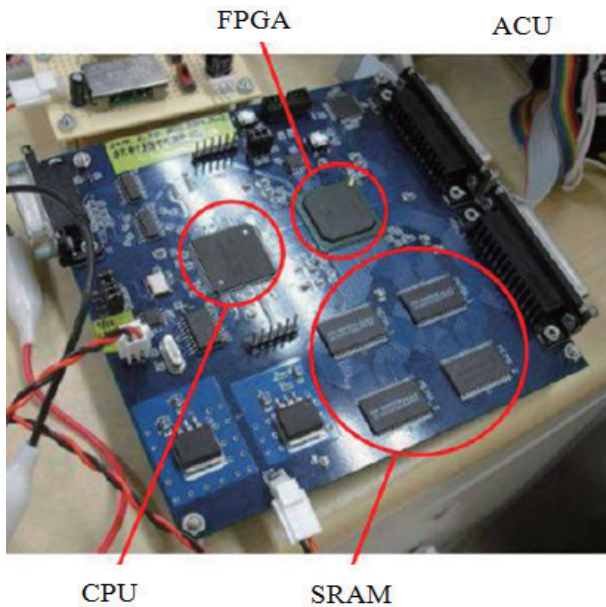


Fig. 10. Data processing electronics.

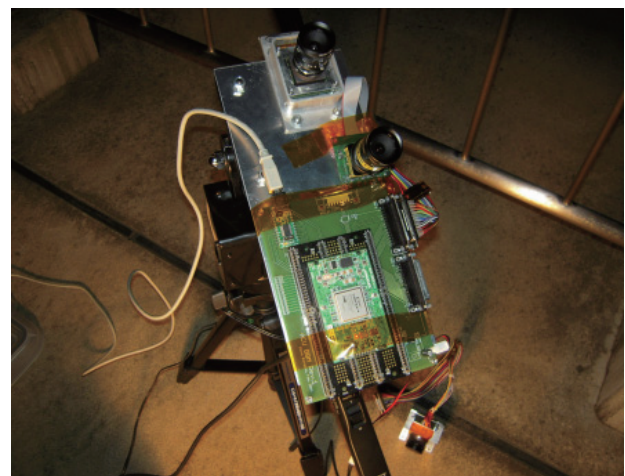


Fig. 13. Field experiment with a functional model.

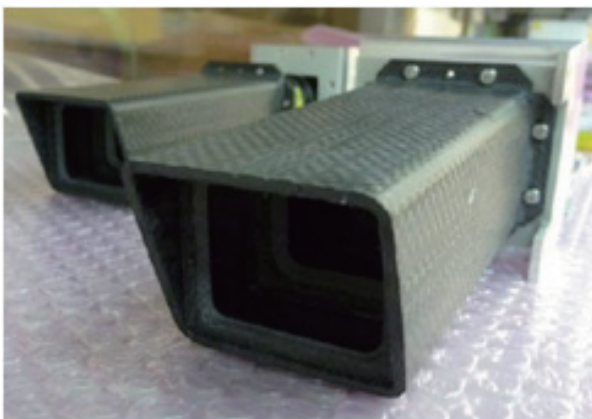


Fig. 11. Star sensor camera head unit.

The simplified block diagram of the internal structure of the ACU relative to star sensor data processing is illustrated in Fig. 12. The design of the PCB of the ACU, selection of the components such as CCD sensor and lens, and the development of the baffle, as well as the system integration were done by Tohoku University.

**5. Functional Evaluation**

The performance of the designed star sensor was evaluated by both simulations and field experiments. In the Fig. 13, a scene of field experiments with a functional model is illustrated. For the performance evaluation, a simple user GUI which runs on PC was developed to control the camera parameters, step-by-step attitude determination processing, and comparison between obtained images and calculated relative star positions according to the output quaternion.

**5.1. Environmental tests**

Various environmental tests were also conducted to verify the performance of the star sensor in space. First of all, radiation tests were repeatedly conducted and appropriate electrical chips on the ACU, the sensor and its electronics, and the lens system were carefully selected as shown in Fig. 14. An amount of total ionizing dose of more than 20 krad was set as the performance requirements for the safe operation of more than 2 years of mission duration. To reduce the radiation degradation/browning of the lens system, a so-called radiation blocker window made of synthetic silica is applied.

Secondly the performance against vibration conditions was evaluated as illustrated in Fig. 15 together with the integrated engineering model into the satellite structure in Fig. 16.

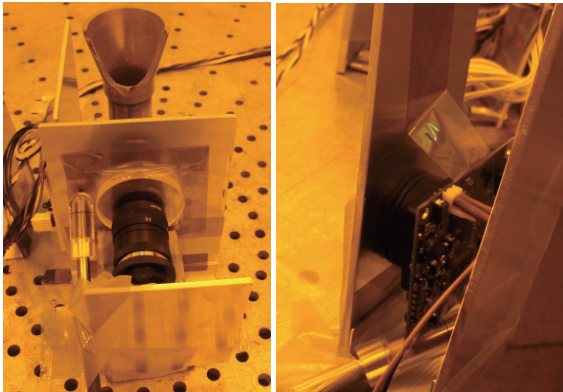


Fig. 14. Radiation tests of star sensor components.

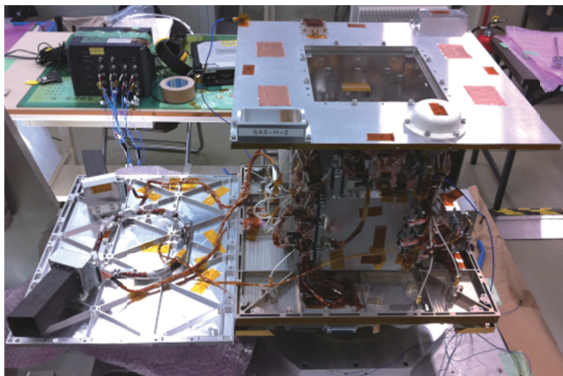


Fig. 15. Vibration tests of engineering model.

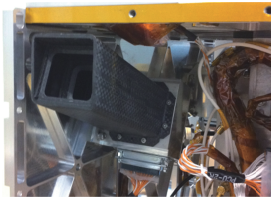


Fig. 16. Integrated sensor unit into the satellite structure.

Some parts such as lens assembly where their less vibration tolerances were revealed were properly reinforced by e. g. bonding adhesives. As the result, the star sensor hardware was verified against the specified launch vibration condition of Japanese H-IIA launcher.

Finally a thermal vacuum test was conducted in the satellite system level as illustrated in Fig. 17. The COTS-based lens assembly was modified so that the trapped air between lenses can escape during the vacuuming process.

### 5.2. Achieved performance

The specification of the developed star sensor can be summarized in Table 1. According to the functional evaluation/verification activities, the achieved attitude knowledge accuracy is determined as about 0.053 deg when the angular velocity is 0 deg/s, and about 0.059 deg in 0.2 deg/s, where the maximal angular velocity of the satellite during the normal operation is defined as less than 0.1 deg/s. The attitude determination process generally takes less than 0.5 s realizing 2 Hz, and sometimes up to 1 s resulting in 1 Hz depending on the observing direction and identified stars in the image.



Fig. 17. System level thermal vacuum test.

Table 1. Star sensor specification.

CCD sensor	651 × 484 pixels
Lens	Focal length: 12 mm Field of view: ≈ 22 deg × 30 deg
Star catalog	Magnitude 4 or brighter
Attitude knowledge accuracy	0.053 deg ( with 0.0 deg/s) 0.059 deg ( with 0.2 deg/s)
Update Frequency	1-2 Hz

## 6. Conclusions and Future Outlook

In this paper, the design and system integration of the star sensor developed for the microsatellite RISING-2 at the Tohoku University was briefly described. The star mapping and attitude determination algorithm with pyramid technique is introduced and its mathematical background is summarized. The developed star sensor is based on COTS products and the design and development were done by Tohoku University. According to the functional evaluation and environmental tests, it became clear that the attitude knowledge of the developed star sensor fulfils the requirements.

As future outlook, one can conclude that the attitude knowledge shall be considerably improved so that the star sensor can be applied to other future satellite missions with higher performances. For this purpose the resolution of the CCD sensor can be improved and a smaller field of view can be selected for the lens. As the result, the star catalog shall include more number of star pair entries and the design of the baffle needs to be improved in order to identify stars with less magnitude. The established knowledge in this research will become the basis for development of high accuracy star sensors for future demanding microsatellite missions.

## References

- 1) Mortari, D., Samaan, M. A., Bruccoleri, C. and Junkins J. L.: The Pyramid Star Identification Technique. *Navigation*, **51**, 3 (2004), pp.171-183.
- 2) Spratling, B. and Mortari, D.: A Survey on Star Identification Algorithms. *Algorithms*, Special Issue: Sensor Algorithms, **2**, 1 (2009), pp.93-107.
- 3) Markley, F. L.: Fast Quaternion Attitude Estimation from Two Vector Observations, *Journal of Guidance, Control and Dynamics*, **25**, 2 (2002), pp. 411-414.